Loss of Function of WFS1 Causes ER Stress-Mediated Inflammation in Pancreatic Beta-Cells

Shuntaro Morikawa[1,2], Lindsey Blacher[1], Chinyere Onwumere[1] and Fumihiko Urano[1,3]*

[1] Department of Medicine, Division of Endocrinology, Metabolism, and Lipid Research, Washington University School of Medicine, St. Louis, MO, United States, [2] Department of Pediatrics, Graduate School of Medicine, Hokkaido University, Sapporo, Japan, [3] Department of Pathology and Immunology, Washington University School of Medicine, St. Louis, MO, United States

Wolfram syndrome is a rare genetic disorder characterized by juvenile-onset diabetes mellitus, optic nerve atrophy, hearing loss, diabetes insipidus, and progressive neurodegeneration. Pathogenic variants in the *WFS1* gene are the main causes of Wolfram syndrome. *WFS1* encodes a transmembrane protein localized to the endoplasmic reticulum (ER) and regulates the unfolded protein response (UPR). Loss of function of *WFS1* leads to dysregulation of insulin production and secretion, ER calcium depletion, and cytosolic calpains activation, resulting in activation of apoptotic cascades. Although the terminal UPR has been shown to induce inflammation that accelerates pancreatic β-cell dysfunction and death in diabetes, the contribution of pancreatic β-cell inflammation to the development of diabetes in Wolfram syndrome has not been fully understood. Here we show that *WFS1*-deficiency enhances the gene expression of pro-inflammatory cytokines and chemokines, leading to cytokine-induced ER-stress and cell death in pancreatic β-cells. PERK and IRE1α pathways mediate high glucose-induced inflammation in a β-cell model of Wolfram syndrome. M1-macrophage infiltration and hypervascularization are seen in the pancreatic islets of *Wfs1* whole-body knockout mice, demonstrating that WFS1 regulates anti-inflammatory responses in pancreatic β-cells. Our results indicate that inflammation plays an essential role in the progression of β-cell death and diabetes in Wolfram syndrome. The pathways involved in ER stress-mediated inflammation provide potential therapeutic targets for the treatment of Wolfram syndrome.

Keywords: Wolfram syndrome, inflammation, diabetes, macrophage, endoplasmic reticulum stress, unfolded protein response

INTRODUCTION

Wolfram syndrome is a rare genetic disorder characterized by juvenile-onset diabetes mellitus, optic nerve atrophy, hearing loss, and progressive neurodegeneration (1–6). Most cases of Wolfram syndrome are caused by pathogenic variants in the *WFS1* gene, which encodes a transmembrane protein localized to the endoplasmic reticulum (ER) (7). WFS1 regulates ER calcium homeostasis, and its dysfunction causes the accumulation of unfolded/misfolded proteins in the ER (referred to as

ER stress). Terminal ER stress mediates cell death in pancreatic β-cells and neuronal cells, which is thought to be the mechanism of Wolfram syndrome development (8–10).

ER stress occurs even under physiological conditions, as protein folding in the ER is an error-prone process. To maintain cellular and organ homeostasis, the unfolded protein response (UPR) determines the cell's fate by sensing adaptive or terminal ER stress (11). The induction of adaptive UPR that leads to cell survival, or the initiation of terminal UPR that leads to cell apoptosis, is regulated by the molecular components of the UPR: inositol-requiring transmembrane kinase/endoribonuclease 1α (IRE1α), protein kinase RNA-like endoplasmic reticulum kinase (PERK), and activating transcription factor 6 (ATF6).

Increasing evidence indicates the cross-talk between UPR and inflammation, that is, a pathogen-free "sterile" inflammatory response triggered by excess ER stress (12). Among the UPR signaling pathways, the IRE1α pathway is known to degrade IκB, a specific inhibitor of nuclear factor-κB (NF-κB), which is a family of transcription factors that regulates the gene expression of pro-inflammatory cytokines (13). In addition, the PERK pathway is known to suppress IκB translation (14). These UPR pathways regulate the nuclear translocation of NF-κB and are the molecular mechanisms linking terminal ER stress and sterile inflammation (14). Since pancreatic β-cells are heavily loaded with protein synthesis and proinsulin is prone to misfold, ER stress is closely associated with the pathogenesis of diabetes (15). Moreover, increasing evidence suggests that ER stress-induced sterile inflammation is involved in the progression of type 2 diabetes (15–17).

We previously showed that WFS1 dysfunction causes terminal ER stress-mediated pancreatic β-cell death (18).

However, the role of inflammation in Wolfram syndrome and its relationship with WFS1 has not been fully elucidated. In this study, we hypothesized that terminal ER stress and inflammation in pancreatic β-cells might accelerate the progression of diabetes in Wolfram syndrome. Our findings reveal islet-localized inflammation in Wolfram syndrome models and suggest that WFS1 functions to regulate sterile inflammation in pancreatic β-cells. Supplementing our previous model that shows the relationship between WFS1 and ER stress-induced pancreatic β-cell death, here we provide new evidence showing that islet-localized inflammation accelerates the progression of diabetes in Wolfram syndrome.

RESULTS

Loss of Function of WFS1 Induces Sterile Inflammation in Pancreatic β-Cells

To investigate whether WFS1 dysfunction leads to sterile inflammation via terminal ER stress in pancreatic β-cells, we first examined apoptosis and pro-inflammatory cytokine gene expression levels in Wfs1 knockdown INS-1E cells. In this in vitro Wolfram syndrome model, cleaved caspase-3 levels were increased, suggesting activation of apoptosis (**Figures 1A, B**). Furthermore, the gene expression levels of pro-inflammatory cytokines [Il-1β, Il-6, and Cxcl1(Il-8)] and Chop were significantly upregulated (**Figure 1C**). These results indicate that WFS1 plays a role in regulating ER stress-mediated cell death and pro-inflammatory cytokine gene expression.
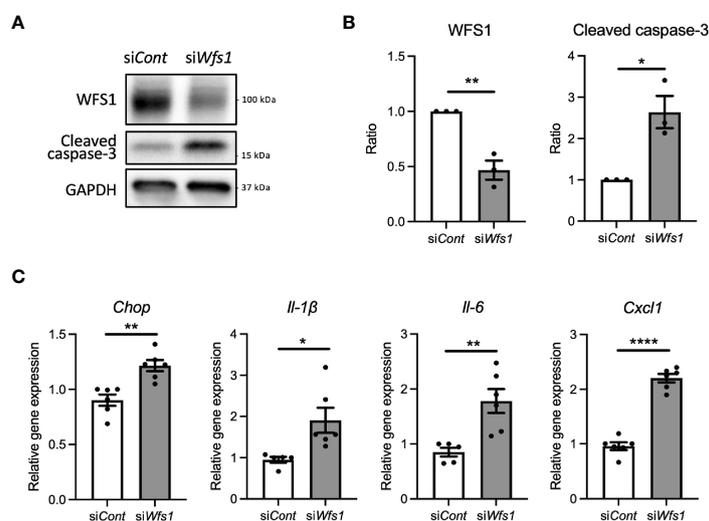

FIGURE 1 | Cell apoptosis and expression of pro-inflammatory cytokine genes are upregulated in Wfs1-deficient pancreatic β-cells. **(A, B)** INS-1E cells were transfected with scrambled siRNA (siCont) or siRNA targeting rat Wfs1 (siWfs1). WFS1 and cleaved caspase-3 protein expression levels were analyzed by immunoblot. Representative images are shown in **(A)**, and quantitative analysis results are shown in **(B)** (n=3, normalized to GAPDH). **(C)** mRNA expression levels of Chop, Il-1β, Il-6, and Cxcl1 (Il-8) in INS-1E cells treated with siCont or siWfs1 normalized to 18srRNA (n=5-6). Data are shown as mean ± SEM, *P < 0.05, **P < 0.005, ****P < 0.0001.

Pro-inflammatory Cytokine Gene Expression Is Enhanced by High-Glucose Stimulation in Pancreatic β-Cell Models of Wolfram Syndrome

Diabetes, caused by ER stress-mediated pancreatic β-cell apoptosis, is one of the major and early manifestations of Wolfram syndrome (1, 19), suggesting that pancreatic β-cells of Wolfram syndrome patients are exposed to hyperglycemia for extended time periods. Therefore, we investigated how WFS1-deficient pancreatic β-cells produce pro-inflammatory cytokines under a chronic high-glucose environment. First, we examined the influence of chronic high-glucose conditions on cell death and ER stress using *Wfs1*-knockout INS-1 832/13 cells (*Wfs1*-KO INS-1 cells) (**Figure 2A**). These *Wfs1*-KO INS-1 cells possess the

characteristics of pancreatic β-cells in Wolfram syndrome: thapsigargin intolerance and mitochondrial dysfunction (20) (**Figure S1**). *Wfs1*-KO INS-1 cells treated with high glucose showed elevated proinsulin expression, increased caspase-3/7 activity, decreased cell viability, and increased gene expression of ER stress markers such as *Chop*, *sXbp1*, *Bip*, and *Txnip* compared to wild-type INS-1 832/13 cells (*Wfs1*-WT INS-1 cells) (**Figures 2B–D**). In this condition, the gene expression levels of pro-inflammatory cytokines (*Il-1β*, *Il-6*), chemokine (*Ccl2*), and vascular endothelial growth factor A (*VegfA*) were increased in *Wfs1*-KO INS-1 cells (**Figure 2E**). The chronic high-glucose condition enhanced not only the cell apoptosis but also the expression of pro-inflammatory cytokine genes in *Wfs1*-KO INS-1 cells.
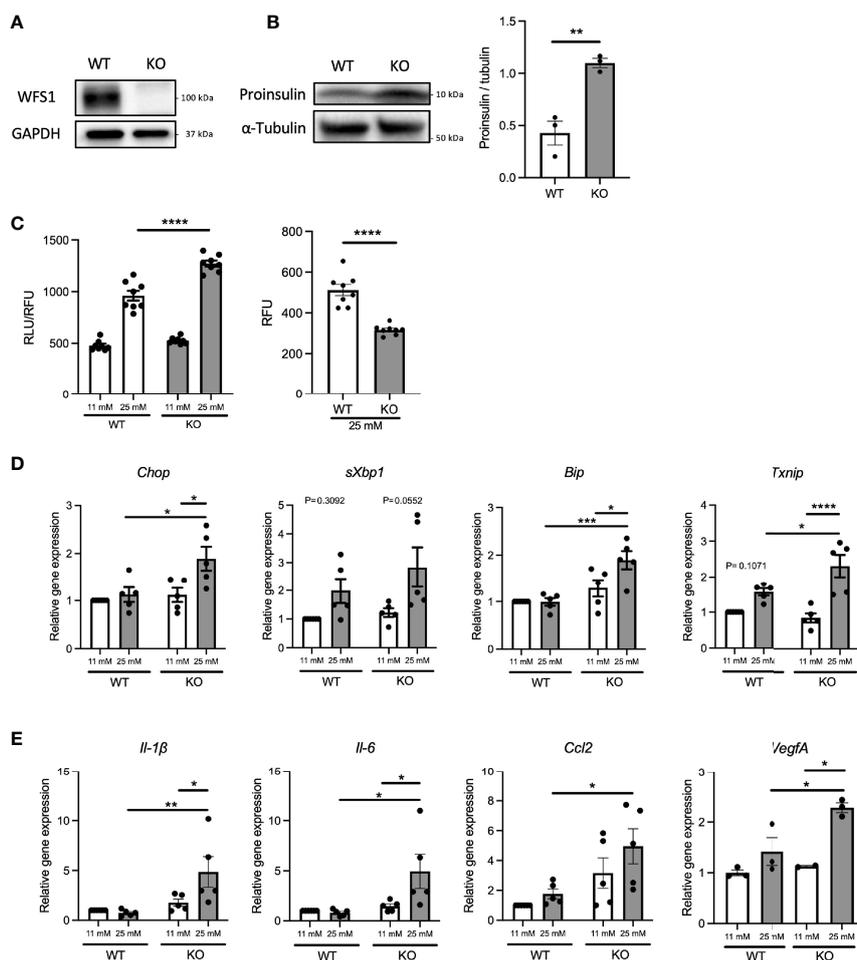

FIGURE 2 | Hyperglycemia upregulates pro-inflammatory cytokine genes expression in *Wfs1*-deficient pancreatic β-cells. **(A)** Immunoblot images of WFS1 in *Wfs1* wild-type (WT) and knockout (KO) INS-1 832/13 cells. **(B)** Left panel: Immunoblot images of proinsulin in WT and KO INS-1 832/13 cells treated with 25 mM glucose for 1 h. Right panel: Proinsulin band intensity was quantified and normalized to tubulin (n=3). **(C)** Left panel: Caspase-3/7 activity normalized to cell viability in WT and KO INS-1 832/13 cells treated with 11 mM or 25 mM glucose for 48 h (n=8). Right panel: Cell viability of WT and KO INS-1 832/13 cells treated with 25 mM glucose for 48 h (n=8) **(D)** mRNA expression levels of *Chop*, *sXbp1*, *Bip*, and *Txnip* in WT or KO INS-1 832/13 cells treated with 11 mM or 25 mM glucose for 48 h (n=3-5), normalized to *18srRNA*. **(E)** The mRNA expression level of *Il-1β*, *Il-6*, *Ccl2*, and *VegfA* in WT and KO INS-1 832/13 cells treated with 11 mM or 25 mM glucose for 48 h (n=3-5), normalized to *18srRNA*. Data are shown as mean ± SEM, *P < 0.05, **P < 0.005, ***P < 0.001, ****P < 0.0001.

Cytokine Treatment Enhances ER Stress-Mediated Cell Apoptosis and Pro-inflammatory Cytokine Gene Expression in Pancreatic β-Cell Models of Wolfram Syndrome

Pro-inflammatory cytokines secreted from pancreatic β-cells are known to act in a paracrine or autocrine manner in type 2 diabetes models (21). Therefore, we hypothesized that the locally secreted cytokines might influence the characteristics of pancreatic β-cells in Wolfram syndrome. To test this idea, we evaluated the cell death and ER stress markers in *Wfs1*-KO INS-1 cells treated with cytokines. *Wfs1*-KO INS-1 cells treated with IFN-γ and IL-1β showed enhanced ER stress-mediated cell death (**Figure 3A**). Furthermore, the gene expression levels of *Il-1β, Il-6*, and *Ccl2* were higher in *Wfs1*-KO INS-1 cells compared to *Wfs1*-WT INS-1 cells (**Figure 3B**). These results indicate that cytokine treatment enhances ER stress-mediated cell death and upregulates the pro-inflammatory cytokine gene expression in *Wfs1*-deficient β-cells.

High-Glucose Induced Pro-inflammatory Cytokine Gene Expression Is Mediated by PERK Pathway in Wolfram Syndrome Pancreatic β-Cells

Next, we investigated the mechanisms underlying the upregulation of pro-inflammatory cytokine gene expressions in *Wfs1*-KO INS-1 cells. We first examined the protein expression level of nuclear-localized NF-κB, which is known to regulate the expression levels of pro-inflammatory cytokines genes (13). We observed enhanced NF-κB nuclear translocation in *Wfs1*-KO INS-1 cells following high-glucose treatment (**Figure 4A**).

We next examined how high-glucose treatment activates the NF-κB pathway. As described above, the downstream pathways of terminal UPR were activated in high-glucose treated *Wfs1*-KO INS-1 cells, enhancing the expression level of ER stress markers such as *Txnip*. TXNIP is known to activate the NLRP3 inflammasome, which leads to caspase-1 activation and IL-1β maturation, and its gene expression is regulated by PERK and IRE1 (22–24). Therefore, to determine whether the terminal UPR pathway enhances the NF-κB signaling pathways, we downregulated PERK and IRE1α in *Wfs1*-KO INS-1 cells. We found that the PERK was activated in *Wfs1*-KO INS-1 cells by high-glucose treatment (**Figure 4B**). Unlike knocking down IRE1α, knocking down PERK suppressed the enhanced expression of pro-inflammatory cytokine genes in high-glucose treated *Wfs1*-KO INS-1 cells (**Figures 4C, D**). These results suggest that the induction of pro-inflammatory cytokine gene expressions in high-glucose treated *Wfs1*-KO INS-1 cells was mainly mediated by the PERK pathway and subsequent NF-κB nuclear translocation. The increased *Txnip* expression in high-glucose treated *Wfs1*-KO INS-1 cells was suppressed by simultaneously knocking down PERK and IRE1α (**Figure 4E**). These results suggest that high-glucose treatment of *Wfs1*-KO-INS-1 cells enhances NF-κB-mediated pro-inflammatory cytokine genes expression *via* the PERK pathway and enhances TXNIP-mediated IL-1β processing through the PERK and IRE1α pathways.

Islet-Localized and Systematic Inflammation in the Wolfram Syndrome Mouse Model

To confirm the findings above, we next investigated whether inflammation occurs in a mouse model of Wolfram syndrome.
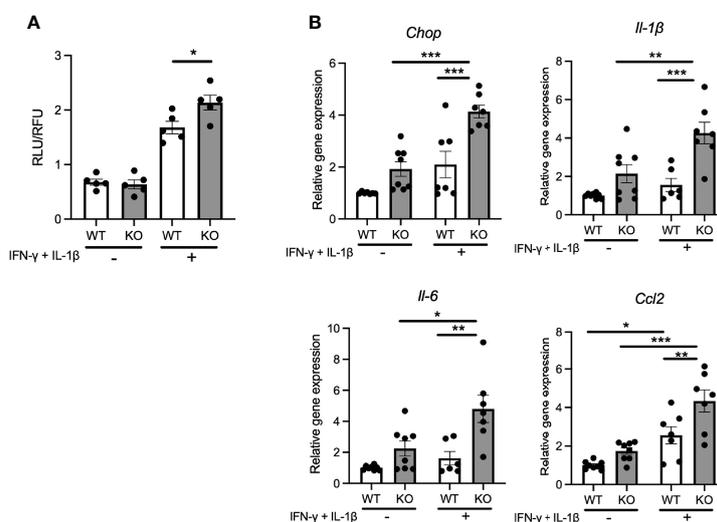

FIGURE 3 | Cytokine treatment causes ER-stress induced cell death and pro-inflammatory cytokines gene upregulation in *Wfs1*-deficient pancreatic β-cells. **(A)** Caspase-3/7 activity normalized to cell viability in *Wfs1* wild-type (WT) and knock-out (KO) INS-1 832/13 cells treated with IFN-γ (50 ng/mL) and IL-1β (50 ng/mL) for 24 h (n=5). **(B)** mRNA expression level of *Chop, Il-1β, Il-6*, and *Ccl2* in WT and KO INS-1 832/13 cells treated with IFN-γ (50 ng/mL) and IL-1β (50 ng/mL) for 24 h (n=6-8), normalized to *18srRNA*. Data are shown as mean ± SEM, *P < 0.05, **P < 0.005, ***P < 0.001.
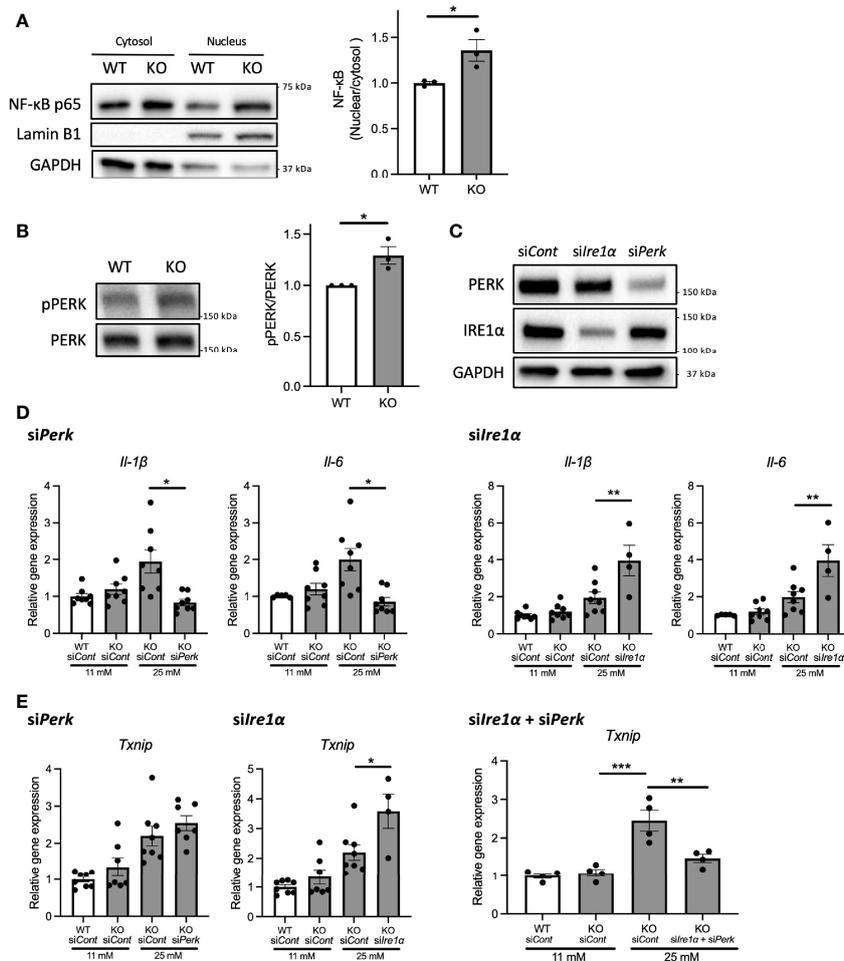
FIGURE 4 | PERK pathway regulates the high-glucose induced pro-inflammatory gene expression in *Wfs1*-deficient pancreatic β-cells. **(A)** Left panel: Immunoblot images of NF-κB p-65 in the cytosolic or nuclear fraction of *Wfs1* wild-type (WT) and knockout (KO) INS-1 832/13 cells. WT and KO INS-1 832/13 cells were treated with 5 mM glucose for 18 h and then with 25 mM glucose for 30 min. Right panel: The ratio of nuclear and cytosolic NF-κB p-65 protein levels (n=3). **(B)** Left panel: Immunoblot images of pPERK and PERK. WT and KO INS-1 832/13 cells were treated with 5 mM for 16 h and then with 25 mM glucose for 24 h. Right panel: pPERK band intensity was quantified and normalized to total PERK (n=3). **(C)** Immunoblot images of PERK and IRE1α in WT and KO INS-1 832/13 cells treated with siRNA against *Perk* or *Ire1α*. **(D)** mRNA expression level of *Il-1β* and *Il-6* normalized to *18srRNA* in WT or KO INS-1 832/13 cells treated with 11 mM or 25 mM glucose for 30 h together with siRNA against *Perk* or *Ire1α* (n=4-8) **(E)** mRNA expression levels of *Txnip* normalized to *18srRNA* in WT and KO INS-1 832/13 cells treated with 11 mM or 25 mM glucose for 6 h together with siRNA against *Ire1α* and *Perk* (n=4). Data are shown in mean ± SEM, *$P < 0.05$, **$P < 0.005$, ***$P < 0.001$.

Although several Wolfram syndrome mouse models have been developed, we used the *Wfs1* whole-body knockout 129S6 mice (*Wfs1*-KO mice) in this study (18, 25), which recapitulate human Wolfram syndrome phenotypes and progressively develop glucose intolerance between 4.5 and 6.5 weeks old that persists through at least 10 months of age (18) (**Figures S2A, B**). It is known to be challenging to isolate a large number of islets from these mice because of their genetic background and small size. Thus, we had to pool islets from several mice or to use imaging mass cytometry for the following experiments. First, we evaluated gene expression levels of pro-inflammatory cytokines and ER stress markers in primary islets from *Wfs1*-wild-type (WT) and *Wfs1*-KO mice. The primary islets isolated from 3-week-old to 12-week-old *Wfs1*-WT or -KO male mice were

pooled and cultured in 30 mM glucose for 3 days. The expression levels of pro-inflammatory cytokine genes (*Il-1β*, *Ccl2*, *Il-6*) and ER stress markers (*Bip*, *sXbp1*, *Txnip*, *Chop*) tended to be higher in *Wfs1*-KO primary islets than in control islets. However, there was a large variation among the samples, and the difference was not statistically significant (data not shown). To further investigate the relationship between WFS1 and islet-localized inflammation, we collected the pancreatic tissues from mature-adult (16-week-old) and middle-aged (10-month-old) *Wfs1*-WT and *Wfs1*-KO mice and examined whether macrophages infiltrate the islets. Pancreatic tissue sections from each age were stained with Iba1, a marker for M1/M2 macrophage. Although there were no significant differences in 16-week-old mice, higher Iba1 density was

observed in *Wfs1*-KO mice islets at 10 months age-old (**Figures 5A, B**). To further evaluate the character of these islet-resident macrophages, we performed imaging mass cytometry (IMC) on the *Wfs1*-KO mice pancreatic sections. The intra-islet macrophages in *Wfs1*-KO mice pancreatic islets expressed CD68 and IL-1β, indicating inflammatory M1-like characteristics (**Figure 5C**). There was also strong fibrosis in the islets of *Wfs1*-KO mice (**Figures 5D, E**), previously described as the hallmark of chronic inflammation in the diabetic islets (26). Together, these findings indicate the presence of inflammation in the *Wfs1*-KO mice islets.

To examine whether the inflammation was also present in other tissues, we assessed cytokine levels in serum and bone marrow-derived macrophages of *Wfs1*-KO mice. Serum cytokine levels, notably interferon gamma-induced protein 10 (IP-10, CXCL10), was elevated in *Wfs1*-KO mice (**Figure S3**). These results suggest that the inflammation in these *Wfs1*-KO mice was

not limited to the pancreatic islets. Although the high-glucose condition did not alter the gene expression levels of pro-inflammatory cytokines in bone marrow-derived macrophages (**Figures S4A, B**), advanced glycation end products (AGE) treatment enhanced *Ccl2* gene expression in bone marrow-derived macrophages of *Wfs1*-KO mice (**Figures S4C, D**).

Hypervascularization in Wolfram Syndrome Mouse Model Islets

In *Wfs1*-KO INS-1 cells, we observed that high-glucose treatment enhanced *VegfA* gene expression (**Figure 2E**). VEGFA, an angiogenic factor, is expressed in the mouse islet and regulates vascular growth and permeability (27–29). Therefore, we tested if increased VEGFA expression may cause abnormal angiogenesis in the pancreatic islets of *Wfs1*-KO mice. We evaluated the endothelial cell marker (CD31) in the pancreas of *Wfs1*-WT and *Wfs1*-KO mice. A higher CD31 signal density
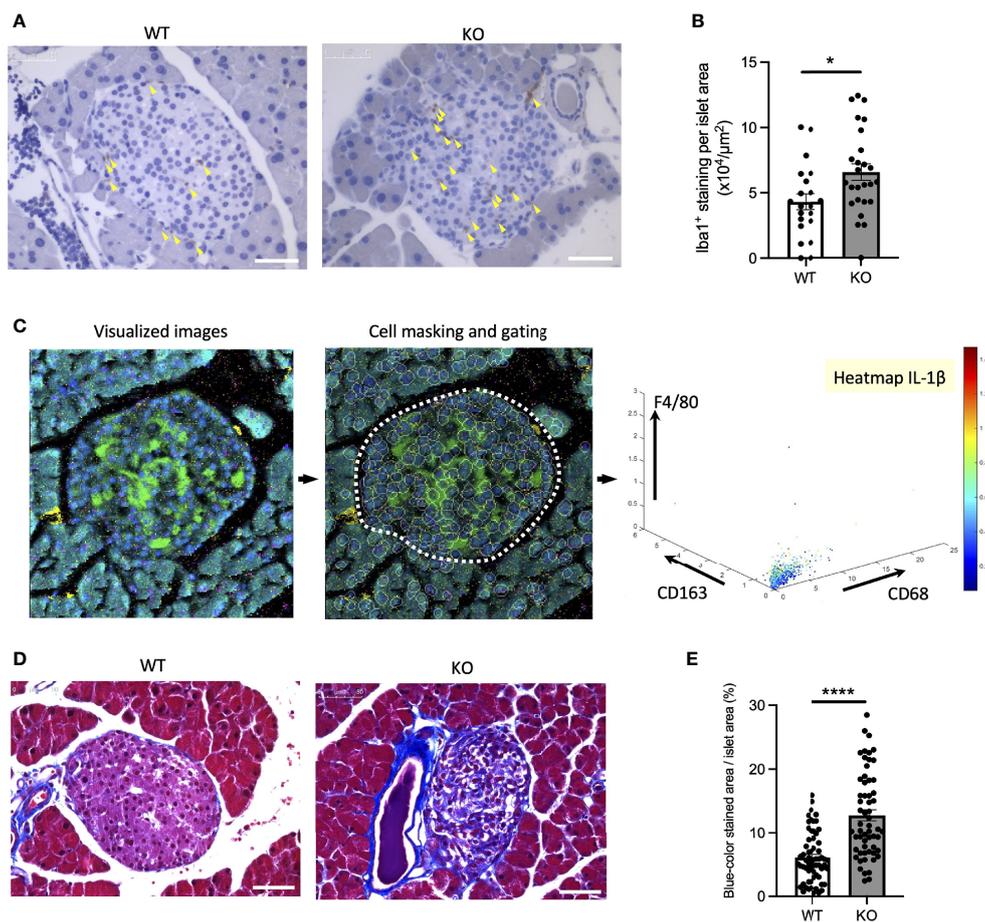

FIGURE 5 | Macrophage infiltration and fibrosis in the Wolfram syndrome mouse model islets. **(A)** Iba1 DAB staining of the islets from *Wfs1* wild-type (WT) and whole-body knockout 129S6 (KO) male mice at 10 months of age. Yellow arrowheads point to the stained macrophages. Scale bars 50 μm. **(B)** The number of Iba1 positive cells was normalized to each islet's area size (WT, n=21; KO, n=28). **(C)** Left panel: Visualized imaging mass cytometry (IMC) image of KO male mouse stained with F4/80 (red), insulin (green), DNA (blue), CD68 (magenta), and CD163 (yellow). Contrast staining was performed with Ruthenium (cyan). Middle panel: cells were masked, and the islet area was gated. Right panel: Scatter plot of F4/80, CD163, and CD68. IL-1β was shown in the heatmap. **(D)** Trichrome-Masson staining of the islets from WT and KO male mice at 10 months of age. Collagen fibers are stained in blue. Scale bars 50 μm. **(E)** The blue-colored area was normalized to each islet's area size (WT, n=33; KO, n=34). Data are shown in mean ± SEM, *P < 0.05, ****P < 0.001.

was observed in *Wfs1*-KO mice islets compared to *Wfs1*-WT mice (**Figures 6A, B**). These results indicate the existence of hypervascularization in the islets of *Wfs1*-KO mice.

DISCUSSION

Although the relationship between the ER stress and pancreatic β-cell death in Wolfram syndrome has been well established, the role of inflammation in the development of Wolfram syndrome remains unknown. This study provides the first evidence indicating that high-glucose and cytokine treatment activate inflammation in pancreatic β-cell model of Wolfram syndrome. We also confirmed the cell-nonautonomous pancreatic β-cell inflammation, including M1-macrophage infiltration in the islets of a mouse model of Wolfram syndrome. In pancreatic β-cells, ER stress and high-glucose conditions enhance the production and secretion of IL-1β, which is characteristic of sterile inflammation (22). Our data demonstrate that the vulnerability to high-glucose and high-cytokine conditions potentiates ER stress and pro-inflammatory cytokine gene expression in WFS1-deficient pancreatic β-cells. We speculate that this environment leads to pancreatic β-cell death, and the consequent chronic hyperglycemia induces sterile inflammation in Wolfram syndrome, causing further pancreatic β-cell loss. This vicious cycle of inflammation and ER stress may accelerate the progression of diabetes in Wolfram syndrome (**Figure 7**). However, this study has not clarified whether WFS1 directly regulates sterile inflammation or whether the expression levels of pro-inflammatory cytokine genes are upregulated even in the absence of terminal ER stress. It has previously been shown that the ER stress level in pancreatic β-cells of the Wolfram syndrome model mouse can be suppressed by Exendin-4, a glucagon-like protein-1 (GLP-1) receptor agonist

(30). We have previously shown that dantrolene sodium reduces serum IL-1β levels in patients with Wolfram syndrome (31). Therefore, the relationship between WFS1-deficiency and sterile inflammation can be further elucidated by assessing the expression levels of pro-inflammatory cytokine genes or ER stress markers in the pancreatic β-cells treated with these therapeutic drugs.

The islet-resident macrophages originated from hematopoietic stem cells and are present at steady-state conditions (32). However, the density of islet-resident macrophages is known to increase in patients with type 2 diabetes and rat and mouse models of type 2 diabetes (33, 34). These islet-resident macrophages express an M1-like transcript signature, and the macrophages infiltrated into the islets trigger subsequent autoimmune responses (34–36). In this study, we show that pancreatic islets in *Wfs1*-KO mice were highly infiltrated with inflammatory M1-macrophages. Therefore, islet-localized inflammation, which has been shown in the type 2 diabetes models, is also present in cell and mouse models of Wolfram syndrome.

Circulating macrophages are known to infiltrate tissues and differentiate into tissue-resident macrophages (37). There are two possible reasons for the increased density of islet-resident macrophages in the Wolfram syndrome mouse model. First, macrophages may respond to cytokines and chemokines that are thought to be secreted from islets, as shown by previous studies (34). Our results show that the pancreatic β-cell model of Wolfram syndrome under hyperglycemia expresses a higher level of *Ccl2* mRNA compared to the wild-type cells. Furthermore, previous studies have reported that the recruitment of circulating macrophages to the islets is dependent on CCL2/CCR2 (33, 38). The second possible reason for the high macrophage infiltration is the increased angiogenesis observed in the Wolfram syndrome model mice islets. In this study, we show that *VegfA* mRNA
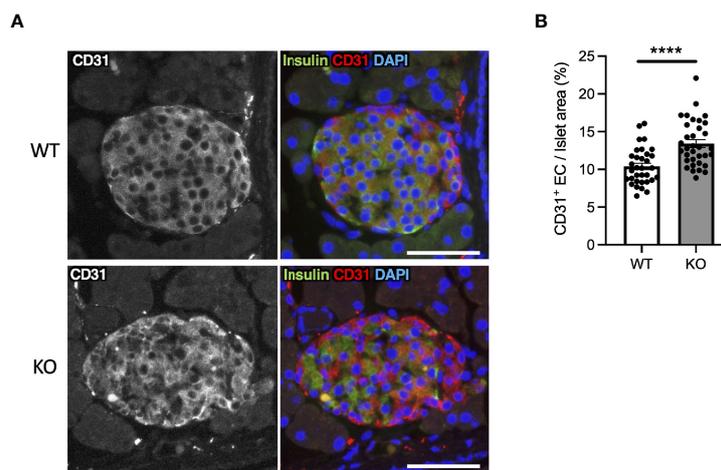

FIGURE 6 | Hypervascularization in the islets of Wolfram syndrome mouse model. **(A)** Representative immunofluorescent images of islets from *Wfs1* wild-type (WT) and whole-body knockout 129S6 (KO) male mice at 10 months of age. Scale bars 50 μm. **(B)** Quantification of endothelial cell marker (CD31) positive area and islet area composition (WT, n=33; KO, n=34). Data are shown as mean ± SEM, ****P < 0.001.
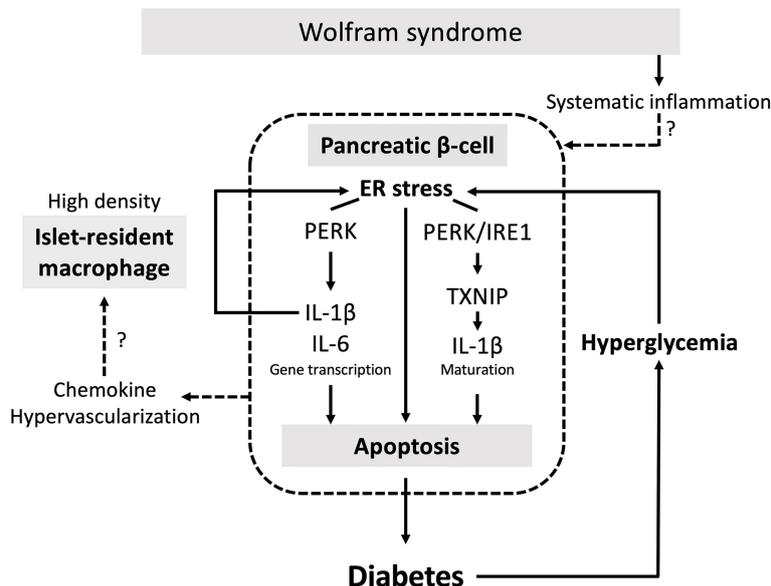
FIGURE 7 | The vicious cycle of inflammation and ER stress accelerates the progression of diabetes in Wolfram syndrome. Schematic of the relationship between ER stress and sterile inflammation in Wolfram syndrome (WS). Diabetes in WS is caused by terminal ER stress-induced pancreatic β-cell apoptosis. Hyperglycemic conditions of *WFS1*-deficient pancreatic β-cells enhance terminal ER stress and induce sterile inflammation. Experimental high-glucose condition induces pro-inflammatory cytokine gene transcription *via* the PERK pathway and enhances TXNIP-mediated IL-1β processing through the PERK and IRE1α pathways. This high-cytokine condition accelerates ER stress-mediated cell death and upregulates the pro-inflammatory cytokine gene expression in *WFS1*-deficient pancreatic β-cells. Secreted chemokines or the hypervascularized environment in the WS islets may cause cell-nonautonomous pancreatic β-cell inflammation, including M1-macrophage infiltration.

expression level was increased in WFS1-deficient β-cells. VEGF-A produced in pancreatic islets plays a critical role in islet angiogenesis (29), and we have previously shown that VEGF-A transcription is regulated by the UPR pathway (39). Islet-resident macrophages and blood vessels are in close contact, and chronic islet hypervascularization leads to progressive macrophage infiltration (28, 40). WFS1-deficient cells are vulnerable to ER stress, which promotes *VegfA* expression, which may lead to hypervascularization and macrophage infiltration in the Wolfram syndrome model mice islets. Further studies are needed to clarify whether intra-islet macrophages are proliferating or whether monocytes are recruited into the islets.

A high-glucose environment is known to induce pro-inflammatory cytokine and chemokine genes in macrophages (41). However, in this study, we show that the expression levels of pro-inflammatory cytokine genes in high-glucose treated bone marrow-derived macrophages were not altered by WFS1 deficiency. These results indicate that the functional contribution of WFS1 in the macrophages is not as significant as in the pancreatic β-cells, possibly because the expression level of WFS1 is lower in macrophages than in the other organs (https://www.proteinatlas.org/ENSG00000109501-WFS1). On the other hand, *Wfs1*-deficient bone marrow-derived macrophages stimulated with AGE showed an increased expression level of the *Ccl2* gene, a marker of M1 macrophages. Since AGE serum levels in Wolfram syndrome model mice increased with age, it is possible that stimulating factors other than blood glucose, including AGE,

alter the transcript signature of macrophages in a model of Wolfram syndrome.

In type 2 diabetes, elevated levels of serum pro-inflammatory cytokines such as IL-1β and IL-6 are predictive disease markers (17, 42, 43). In this study, we showed that inflammatory cytokine levels in the serum of a mouse model of Wolfram syndrome are higher than that of wild-type mice. This result is consistent with the recent studies that showed elevated cytokine levels in Wolfram syndrome patient serum and elevated cytokine production in peripheral blood mononuclear cells (PBMC) isolated from Wolfram syndrome patients (31, 44). The source of the elevated serum cytokines in Wolfram syndrome is still unknown; however, since the pancreatic islets are highly vascularized, systemic inflammation may affect the islet inflammation. It is essential to investigate the contribution to the systematic inflammation in Wolfram syndrome by other tissues and organs such as adipose tissue, liver, and blood cells other than macrophages, which are involved in the inflammation associated with type 2 diabetes. Cells or tissues differentiated from patient-derived iPSCs would provide a better model to study the role of inflammation in Wolfram syndrome (45).

Besides the Wolfram syndrome pancreatic β-cells, sterile inflammation occurs in many other cell types such as oligodendrocytes, hepatocytes, and adipocytes, where the ER is heavily loaded with proteins (12). Symptoms seen in Wolfram syndrome are accompanied not only by diabetes but also by optic nerve atrophy and neurodegeneration, whose pathogenic

mechanisms are not fully understood. Therefore, this study suggests that the metabolic factors, including hyperglycemia, inflammatory cytokines, and AGE, may contribute to the progression of Wolfram syndrome symptoms in a cell-nonautonomous manner.

In summary, our study identifies sterile inflammation as a new pathological mechanism in Wolfram syndrome. In Wolfram syndrome model mice, islets are highly infiltrated with macrophages, suggesting that the vicious cycle of ER stress and inflammation accelerates the progression of diabetes in a cell-autonomous and cell-nonautonomous manner. A deeper understanding of the pathophysiology of Wolfram syndrome is essential for developing novel therapeutic targets for the disease. As the inflammation-targeted therapies have been tried in type 2 diabetes (46), the findings from this study may also be applicable not only to diabetes in Wolfram syndrome but also to other manifestations such as optic atrophy and neurodegeneration, which severely impair the quality of life of patients with Wolfram syndrome.

MATERIALS AND METHODS

Cell Culture

Wfs1-KO INS-1 832/13 cells were generated in collaboration with Genome Engineering and Induced Pluripotent Stem Cell Center (GEiC) at Washington University in St. Louis as described before (20). INS-1 832/13 cells were cultured in 11 mM glucose RPMI 1640 (Thermo Fisher Scientific, Cat# 11875) supplemented with 10% fetal bovine serum (FBS) (Thermo Fisher Scientific, Cat# 10099141), 1 mM sodium pyruvate (Corning, Cat# 25-000-CI), 90 μM β-mercaptoethanol (MilliporeSigma, Cat# M3148) and 100 U/mL penicillin-streptomycin (Thermo Fisher Scientific, Cat# 15140122). INS-1E cells were cultured in 11 mM RPMI 1640 supplemented with 10% FBS, 1 mM sodium pyruvate, 50 μM β-mercaptoethanol, 2 mM GlutaMAX (Thermo Fisher Scientific, Cat# 35050061), NEAA (Thermo Fisher Scientific, Cat# 11140050), 10 mM HEPES (Corning, Cat# 25-060-CI), and 100 U/mL penicillin-streptomycin. Rat IFN-γ, rat IL-1β (R&D Systems, Cat# 585-IF-100, 501-RL-010), and thapsigargin (MilliporeSigma, Cat# T9033) were used for the treatments.

Wolfram Syndrome Mouse Model and Pancreatic Sample Preparation

129S6 whole body *Wfs1*-knockout mice were a kind gift from Dr. Sulev Kõks (University of Tartu) (25). Amino acids 360-890 of WFS1 protein were replaced with an in-frame NLSLacZNeo cassette. Mouse genotypes were determined using multiplex PCR performed by Transnetyx (Cordova, TN). All animal experiments were performed according to procedures approved by the Institutional Animal Care and Use Committee at the Washington University School of Medicine (Protocol # 20-0334). All mice were housed in a pathogen-free animal facility, and food and water were provided *ad libitum* throughout the study. For the pancreatic section slides, 129S6 whole body *Wfs1*-knockout mice were euthanized in a carbon dioxide chamber followed by

cervical dislocation. The mice were perfused with PBS and 4% paraformaldehyde (PFA) *via* the left ventricle. After perfusion, the pancreas was removed and fixed with 4% PFA for 48 h at 4°C. The fixed pancreas was gradually replaced by ethanol and finally kept in 70% ethanol. Paraffin embedding and sectioning were performed by Histology and Morphology Core at Musculoskeletal Research Center at Washington University in St. Louis. Slides were sectioned at 5 μm thickness. Microscopy imaging was performed using a Leica DM6B (Leica Microsystems, Germany). All quantitative analyses were conducted using Fiji ImageJ in a double-blinded fashion.

Immunostaining

Paraffin-embedded pancreatic section slides were deparaffinized, and antigen retrieval was performed by submerging the slides in 10 mM sodium citrate solution (pH 6.0) for 30 min at 95°C. The tissues were permeabilized with phosphate buffer saline (PBS) containing 0.1% Triton X-100 for 30 min at room temperature. For the DAB stained samples, endogenous peroxidase was quenched using BLOXALL Blocking solution (VECTOR, Cat# SP-6000). Blocking was performed in 2% bovine serum albumin (BSA) for 1 h. The following primary antibodies were diluted in 0.2% BSA and incubated overnight at 4°C: anti-WFS1 (Proteintech, Cat# 1158-1-AP, 1:100), anti-Iba1 (Novus, Cat# NB100-1028, 1:50), anti-CD31 (abcam, Cat# ab124432, 1:100), and Alexa-Fluor 488 conjugated anti-insulin (Invitrogen, Cat# 53-9769-82, 1:100). After washing the primary antibodies 3 times with PBS, the tissues were incubated for 30 min at room temperature with ImmPRESS polymer reagent (VECTOR, Cat# MP-7401-50) for DAB staining, or AlexaFluor 594 donkey anti-rabbit IgG (Invitrogen, Cat# A21207) for immunofluorescent staining, and washed for 2 times with PBS. The color development for DAB staining was performed using peroxidase substrate solution (VECTOR, Cat# SK-4100) following the manufacturer's protocol, and then the nucleus was stained by Vector Hematoxylin QS (VECTOR, Cat# H-3404). Tissues were mounted in Vectamount permanent mounting medium (VECTOR, Cat# H5000-60).

Masson's Trichrome Staining

Deparaffinized and rehydrated slides were immersed in Bouin's solution at 56°C for 1 h. Subsequently, the slides were washed with tap water for 5 min. The washed sections were stained in Weigert's Hematoxylin solution for 10 min and then washed again with tap water for 5 min. Next, the slides were stained in Trichrome solution for 15 min and rinsed in 1% acetic acid for 1 min. Slides were dehydrated in alcohol twice for 1 min each, and sections were cleared in xylene twice for 1 min each. All the Masson's trichrome staining procedures were performed by the Musculoskeletal Research Center at Washington University in St. Louis.

Imaging Mass Cytometry

The antibody staining on formalin-fixed paraffin-embedded (FFPE) mouse pancreatic tissue was performed based on Fluidigm immunohistochemistry protocol. Briefly, the FFPE slides were deparaffinized followed by antigen retrieval using

10 mM sodium citrate (pH 6.0) for 30 min at 96°C. Blocking was performed using metal-free 3% BSA for 45 min prior to the addition of the primary antibody solution. The primary antibodies were anti-F4/80(BM8) (Fluidigm, Cat# 3146008B), anti-CD68(FA-11) (Biolegend, Cat# 137001), anti-CD163 (EPR19518) (Abcam, Cat# ab182422), and anti-IL-1β/IL-1F2 (Novus Biologicals, Cat# NBP1-42767). Metal conjugation was performed using MAXPAR® X8 Multimetal Labeling Kit (Fluidigm, Cat# 201300), and all the antibodies were used in a 1:25 dilution. After overnight incubation of the antibody mixture at 4°C in a humidity chamber, the slide was washed with 0.2% Triton X-100 in PBS and then stained with 0.0025% Ruthenium Red for contrast staining. After the contrast staining, a DNA intercalator for nuclear identification was added. The slides were washed in distilled water and then air-dried before imaging. Antibody conjugation and CyTOF2/Helios imaging were performed by the Immunomonitoring Laboratory (IML) in Bursky Center for Human Immunology & Immunotherapy Programs (CHiiPs) at Washington University in St. Louis. Optimization of the multiplex panel involves assessing dual signal spillover into +1, +2, and +16 channels and lack of signal (false negative). Assessment of signal in other channels was performed using MCD Viewer software and generating a thumbnail image file for each metal channel. The imaging data were converted to TIFF images using HistoCAT++ (ver 3.0.0), and CellProfiler (ver 4.1.3) was used for the cell masking. Image visualization and data analysis were performed using HistoCAT (ver 1.761).

Cell Death Assay

INS-1 832/13 cells were plated on 96-well flat clear bottom white polystyrene plates (Corning, Cat# 3610) and treated with or without the indicated reagents. After the treatment, CellTiter-Fluor Cell Viability Assay (Promega, Cat# G6080) reagent was added directly to cells and incubated for 30 min in the dark. After the fluorescence measurement, Caspase-Glo 3/7 Assay (Promega, Cat# G8090) reagent was added to the cells and incubated for 30 min. Fluorescence for cell viability and luminescence for caspase-3/7 activity was measured using Infinite M1000 plate reader (Tecan). Caspase-3/7 activity was normalized to cell viability according to the manufacturer's protocol.

Immunoblot

Cells were washed in cold PBS and immediately lysed on ice in Mammalian Protein Extraction Reagent (Thermo Fisher Scientific, Cat# 78501) supplemented with 1X cOmplete™ protease inhibitor cocktail (MilliporeSigma, Cat# 11873580001) and 1X PhosSTOP™ phosphatase inhibitor (MilliporeSigma, Cat# 4906845001) before centrifugation at 15,000 rpm for 10 min at 4°C. Nuclear and cytoplasmic extraction was performed using NE-PER™ (Thermo Fisher Scientific, Cat# 78833) according to the manufacturer's protocol. Protein lysates were prepared using 4x Laemmli sample buffer (Bio-Rad Laboratories, Cat# 1610747) heated at 60°C for 15 min. The protein was resolved by SDS-PAGE and transferred to Immobilon-P PVDF membrane [MilliporeSigma, 0.2 μm pore size (Cat# ISEQ20200)

for proinsulin and 0.45 μm pore size for others (Cat# IPVH00010)]. For detecting proinsulin, additional fixation and antigen retrieval steps were performed as reported previously (47). The antibodies used for immunoblotting were anti-WFS1 (Proteintech, Cat# 1158-1-AP), anti-LaminB1 (Proteintech, Cat# 12987-1-AP), and those purchased from Cell Signaling Technology: anti-cleaved caspase-3 (Cat# 9664), anti-insulin (Cat# 8138), anti-pPERK (Cat# 3179), anti-PERK (Cat# 3192), anti-IRE1α (Cat# 32945), anti-NF-κB (Cat# 8242), anti-GAPDH (Cat# 2118), anti-α-tubulin (Cat# 2125), and the secondary antibodies conjugated to horseradish peroxidase. Bands were detected by ECL Select (MilliporeSigma, Cat# RPN2235) and Bio-Rad ChemiDoc MP. Quantitative analyses were conducted using Fiji ImageJ.

Quantitative Real-Time PCR

Total RNA was extracted from INS-1E, INS-1 832/13, or isolated primary mouse macrophages using RNeasy Mini Kit (Qiagen, Cat# 74106) and reverse-transcribed using High-Capacity cDNA Reverse Transcription Kits (Thermo Fisher Scientific, Cat# 4368814). The qPCR was performed in 3-8 replicates for each sample. All the qPCR primer sequences used in this study are listed in **Table S1**.

siRNA

INS-1E or INS-1 832/13 cells were seeded in a 12-well plate and transfected with siRNA using RNAiMAX (Thermo Fisher Scientific, Cat# 13778150). ON-TARGET plus SMARTpool siRNA was used for knocking down rat *Wfs1* (Dharmacon, Cat# L-087932-02). The siRNA against rat *Perk*, *Ire1α*, and non-targeting siRNA were purchased from MilliporeSigma (rat *Perk*, SASI_Rn01_00064452; rat *Ire1α*, SASI_Rn02_00372535; SIC001 for non-targeting). Each siRNA was used in 40 nM concentration, and RNAiMAX was used 1.0 μL against 1 pmol of siRNA. The cells were collected for the analysis 48 h after the siRNA transfection.

Statistical Analysis

All statistics were performed using GraphPad Prism 9. Statistical analysis was performed by unpaired two-tailed Student's t-test or one-way ANOVA followed by Tukey's multiple comparisons test. $P < 0.05$ was considered statistically significant.

DATA AVAILABILITY STATEMENT

The original contributions presented in the study are included in the article/**Supplementary Material**. Further inquiries can be directed to the corresponding author.

ETHICS STATEMENT

All animal experiments were performed according to procedures approved by the Institutional Animal Care and Use Committee

at the Washington University School of Medicine (Protocol # 20-0334).

SUPPLEMENTARY MATERIAL

The Supplementary Material for this article can be found online at: https://www.frontiersin.org/articles/10.3389/fendo.2022.849204/full#supplementary-material

REFERENCES

1. Urano F. Wolfram Syndrome: Diagnosis, Management, and Treatment. *Curr Diabetes Rep* (2016) 16(1):6. doi: 10.1007/s11892-015-0702-6

2. de Heredia ML, Cleries R, Nunes V. Genotypic Classification of Patients With Wolfram Syndrome: Insights Into the Natural History of the Disease and Correlation With Phenotype. *Genet Med* (2013) 15(7):497–506. doi: 10.1038/gim.2012.180

3. Barrett TG, Bundey SE, Macleod AF. Neurodegeneration and Diabetes: UK Nationwide Study of Wolfram (DIDMOAD) Syndrome. *Lancet* (1995) 346:1458–63. doi: 10.1016/S0140-6736(95)92473-6

4. Marshall BA, Permutt MA, Paciorkowski AR, Hoekel J, Karzon R, Wasson J, et al. Phenotypic Characteristics of Early Wolfram Syndrome. *Orphanet J Rare Dis* (2013) 8(1):64. doi: 10.1186/1750-1172-8-64

5. Abreu D, Urano F. Current Landscape of Treatments for Wolfram Syndrome. *Trends Pharmacol Sci* (2019) 40(10):711–4. doi: 10.1016/j.tips.2019.07.011

6. Ray MK, Chen L, White NH, Ni R, Hershey T, Marshall BA. Longitudinal Progression of Diabetes Mellitus in Wolfram Syndrome: The Washington University Wolfram Research Clinic Experience. *Pediatr Diabetes* (2022) 23(2):212–8. doi: 10.1111/pedi.13291

7. Inoue H, Tanizawa Y, Wasson J, Behn P, Kalidas K, Bernal-Mizrachi E, et al. A Gene Encoding a Transmembrane Protein is Mutated in Patients With Diabetes Mellitus and Optic Atrophy (Wolfram Syndrome). *Nat Genet* (1998) 20:143–8. doi: 10.1038/2441

8. Lu S, Kanekura K, Hara T, Mahadevan J, Spears LD, Oslowski CM, et al. A Calcium-Dependent Protease as a Potential Therapeutic Target for Wolfram Syndrome. *Proc Natl Acad Sci* (2014) 111(49):E5292–301. doi: 10.1073/pnas.1421055111

9. Fonseca SG, Ishigaki S, Oslowski CM, Lu S, Lipson KL, Ghosh R, et al. Wolfram Syndrome 1 Gene Negatively Regulates ER Stress Signaling in Rodent and Human Cells [Research Support, N.I.H., Extramural Research Support, Non-U.S. Gov't]. *J Clin Invest* (2010) 120(3):744–55. doi: 10.1172/JCI39678

10. Fonseca SG, Fukuma M, Lipson KL, Nguyen LX, Allen JR, Oka Y, et al. WFS1 is a Novel Component of the Unfolded Protein Response and Maintains Homeostasis of the Endoplasmic Reticulum in Pancreatic Beta-Cells [Research Support, N.I.H., Extramural Research Support, Non-U.S. Gov't]. *J Biol Chem* (2005) 280(47):39609–15. doi: 10.1074/jbc.M507426200

11. Hetz C, Papa FR. The Unfolded Protein Response and Cell Fate Control. *Mol Cell* (2018) 69(2):169–81. doi: 10.1016/j.molcel.2017.06.017

12. Zhang K, Kaufman RJ. From Endoplasmic-Reticulum Stress to the Inflammatory Response. *Nature* (2008) 454(7203):455–62. doi: 10.1038/nature07203

13. Liu T, Zhang L, Joo D, Sun SC. NF-kappaB Signaling in Inflammation. *Signal Transduct Target Ther* (2017) 2:17023. doi: 10.1038/sigtrans.2017.23

14. Garg AD, Kaczmarek A, Krysko O, Vandenabeele P, Krysko DV, Agostinis P. ER Stress-Induced Inflammation: Does it Aid or Impede Disease Progression? *Trends Mol Med* (2012) 18(10):589–98. doi: 10.1016/j.molmed.2012.06.010

15. Yong J, Johnson JD, Arvan P, Han J, Kaufman RJ. Therapeutic Opportunities for Pancreatic Beta-Cell ER Stress in Diabetes Mellitus. *Nat Rev Endocrinol* (2021) 17(8):455–67. doi: 10.1038/s41574-021-00510-4

16. Eguchi K, Nagai R. Islet Inflammation in Type 2 Diabetes and Physiology. *J Clin Invest* (2017) 127(1):14–23. doi: 10.1172/JCI88877

17. Donath MY, Shoelson SE. Type 2 Diabetes as an Inflammatory Disease. *Nat Rev Immunol* (2011) 11(2):98–107. doi: 10.1038/nri2925

18. Abreu D, Asada R, Revilla JMP, Lavagnino Z, Kries K, Piston DW, et al. Wolfram Syndrome 1 Gene Regulates Pathways Maintaining Beta-Cell Health and Survival. *Lab Invest* (2020) 100(6):849–62. doi: 10.1038/s41374-020-0408-5

19. De Franco E, Flanagan SE, Yagi T, Abreu D, Mahadevan J, Johnson MB, et al. Dominant ER Stress-Inducing WFS1 Mutations Underlie a Genetic Syndrome of Neonatal/Infancy-Onset Diabetes, Congenital Sensorineural Deafness, and Congenital Cataracts. *Diabetes* (2017) 66(7):2044–53. doi: 10.2337/db16-1296

20. Nguyen LD, Fischer TT, Abreu D, Arroyo A, Urano F, Ehrlich BE. Calpain Inhibitor and Ibudilast Rescue Beta Cell Functions in a Cellular Model of Wolfram Syndrome. *Proc Natl Acad Sci USA* (2020). doi: 10.1073/pnas.2007136117

21. Donath MY, Boni-Schnetzler M, Ellingsgaard H, Halban PA, Ehses JA. Cytokine Production by Islets in Health and Diabetes: Cellular Origin, Regulation and Function. *Trends Endocrinol Metab: TEM* (2010) 21 (5):261–7. doi: 10.1016/j.tem.2009.12.010

22. Oslowski CM, Hara T, O'Sullivan-Murphy B, Kanekura K, Lu S, Hara M, et al. Thioredoxin-Interacting Protein Mediates ER Stress-Induced Beta Cell Death Through Initiation of the Inflammasome [Research Support, N.I.H., Extramural Research Support, Non-U.S. Gov't]. *Cell Metab* (2012) 16 (2):265–73. doi: 10.1016/j.cmet.2012.07.005

23. Lerner AG, Upton JP, Praveen PV, Ghosh R, Nakagawa Y, Igbaria A, et al. IRE1alpha Induces Thioredoxin-Interacting Protein to Activate the NLRP3 Inflammasome and Promote Programmed Cell Death Under Irremediable ER Stress [Research Support, N.I.H., Extramural Research Support, Non-U.S. Gov't]. *Cell Metab* (2012) 16(2):250–64. doi: 10.1016/j.cmet.2012.07.007

24. Shalev A. Minireview: Thioredoxin-Interacting Protein: Regulation and Function in the Pancreatic Beta-Cell. *Mol Endocrinol* (2014) 28(8):1211–20. doi: 10.1210/me.2014-1095

25. Koks S, Soomets U, Paya-Cano JL, Fernandes C, Luuk H, Plaas M, et al. Wfs1 Gene Deletion Causes Growth Retardation in Mice and Interferes With the Growth Hormone Pathway. *Physiol Genomics* (2009) 37(3):249–59. doi: 10.1152/physiolgenomics.90407.2008

26. Homo-Delarche F, Calderari S, Irminger JC, Gangnerau MN, Coulaud J, Rickenbach K, et al. Islet Inflammation and Fibrosis in a Spontaneous Model of Type 2 Diabetes, the GK Rat. *Diabetes* (2006) 55(6):1625–33. doi: 10.2337/db05-1526

27. Brissova M, Aamodt K, Brahmachary P, Prasad N, Hong JY, Dai C, et al. Islet Microenvironment, Modulated by Vascular Endothelial Growth Factor-A Signaling, Promotes Beta Cell Regeneration. *Cell Metab* (2014) 19(3):498–511. doi: 10.1016/j.cmet.2014.02.001

28. Agudo J, Ayuso E, Jimenez V, Casellas A, Mallol C, Salavert A, et al. Vascular Endothelial Growth Factor-Mediated Islet Hypervascularization and Inflammation Contribute to Progressive Reduction of Beta-Cell Mass. *Diabetes* (2012) 61(11):2851–61. doi: 10.2337/db12-0134

29. Brissova M, Shostak A, Shiota M, Wiebe PO, Poffenberger G, Kantz J, et al. Pancreatic Islet Production of Vascular Endothelial Growth Factor-A Is Essential for Islet Vascularization, Revascularization, and Function. *Diabetes* (2006) 55(11):2974–85. doi: 10.2337/db06-0690

30. Kondo M, Tanabe K, Amo-Shiinoki K, Hatanaka M, Morii T, Takahashi H, et al. Activation of GLP-1 Receptor Signalling Alleviates Cellular Stresses and Improves Beta Cell Function in a Mouse Model of Wolfram Syndrome. *Diabetologia* (2018) 61(10):2189–201. doi: 10.1007/s00125-018-4679-y

31. Abreu D, Stone SI, Pearson TS, Bucelli RC, Simpson AN, Hurst S, et al. A Phase Ib/IIa Clinical Trial of Dantrolene Sodium in Patients With Wolfram Syndrome. *JCI Insight* (2021) 6(15):e145188. doi: 10.1172/jci.insight.145188

32. Calderon B, Carrero JA, Ferris ST, Sojka DK, Moore L, Epelman S, et al. The Pancreas Anatomy Conditions the Origin and Properties of Resident Macrophages. *J Exp Med* (2015) 212(10):1497–512. doi: 10.1084/jem.20150496

33. Ying W, Lee YS, Dong Y, Seidman JS, Yang M, Isaac R, et al. Expansion of Islet-Resident Macrophages Leads to Inflammation Affecting Beta Cell Proliferation and Function in Obesity. *Cell Metab* (2019) 29(2):457–474 e5. doi: 10.1016/j.cmet.2018.12.003

34. Ehses JA, Perren A, Eppler E, Ribaux P, Pospisilik JA, Maor-Cahn R, et al. Increased Number of Islet-Associated Macrophages in Type 2 Diabetes. *Diabetes* (2007) 56(9):2356–70. doi: 10.2337/db06-1650

35. Carrero JA, McCarthy DP, Ferris ST, Wan X, Hu H, Zinselmeyer BH, et al. Resident Macrophages of Pancreatic Islets Have a Seminal Role in the Initiation of Autoimmune Diabetes of NOD Mice. *Proc Natl Acad Sci USA* (2017) 114(48):E10418–27. doi: 10.1073/pnas.1713543114

36. Ferris ST, Zakharov PN, Wan X, Calderon B, Artyomov MN, Unanue ER, et al. The Islet-Resident Macrophage is in an Inflammatory State and Senses Microbial Products in Blood. *J Exp Med* (2017) 214(8):2369–85. doi: 10.1084/jem.20170074

37. Ginhoux F, Jung S. Monocytes and Macrophages: Developmental Pathways and Tissue Homeostasis. *Nat Rev Immunol* (2014) 14(6):392–404. doi: 10.1038/nri3671

38. Martin AP, Rankin S, Pitchford S, Charo IF, Furtado GC, Lira SA. Increased Expression of CCL2 in Insulin-Producing Cells of Transgenic Mice Promotes Mobilization of Myeloid Cells From the Bone Marrow, Marked Insulitis, and Diabetes. *Diabetes* (2008) 57(11):3025–33. doi: 10.2337/db08-0625

39. Ghosh R, Lipson KL, Sargent KE, Mercurio AM, Hunt JS, Ron D, et al. Transcriptional Regulation of VEGF-A by the Unfolded Protein Response Pathway [Research Support, N.I.H., Extramural Research Support, Non-U.S. Gov't]. *PloS One* (2010) 5(3):e9575. doi: 10.1371/journal.pone.0009575

40. Zinselmeyer BH, Vomund AN, Saunders BT, Johnson MW, Carrero JA, Unanue ER. The Resident Macrophages in Murine Pancreatic Islets are Constantly Probing Their Local Environment, Capturing Beta Cell Granules and Blood Particles. *Diabetologia* (2018) 61(6):1374–83. doi: 10.1007/s00125-018-4592-4

41. Shanmugam N, Reddy MA, Guha M, Natarajan R. High Glucose-Induced Expression of Proinflammatory Cytokine and Chemokine Genes in Monocytic Cells. *Diabetes* (2003) 52(5):1256–64. doi: 10.2337/diabetes.52.5.1256

42. Spranger J, Kroke A, Mohlig M, Hoffmann K, Bergmann MM, Ristow M, et al. Inflammatory Cytokines and the Risk to Develop Type 2 Diabetes: Results of the Prospective Population-Based European Prospective Investigation Into Cancer and Nutrition (EPIC)-Potsdam Study. *Diabetes* (2003) 52(3):812–7. doi: 10.2337/diabetes.52.3.812

43. Pradhan AD, Manson JE, Rifai N, Buring JE, Ridker PM. C-Reactive Protein, Interleukin 6, and Risk of Developing Type 2 Diabetes Mellitus. *JAMA* (2001) 286(3):327–34. doi: 10.1001/jama.286.3.327

44. Panfili E, Mondanelli G, Orabona C, Belladonna ML, Gargaro M, Fallarino F, et al. Novel Mutations in the WFS1 Gene are Associated With Wolfram Syndrome and Systemic Inflammation. *Hum Mol Genet* (2021) 30(3-4):265–76. doi: 10.1093/hmg/ddab040

45. Maxwell KG, Augsornworawat P, Velazco-Cruz L, Kim MH, Asada R, Hogrebe NJ, et al. Gene-Edited Human Stem Cell-Derived Beta Cells From a Patient With Monogenic Diabetes Reverse Preexisting Diabetes in Mice. *Sci Trans Med* (2020) 12(540):eaax9106. doi: 10.1126/scitranslmed.aax9106

46. Rehman A, Pacher P, Hasko G. Role of Macrophages in the Endocrine System. *Trends Endocrinol Metab* (2021) 32(4):238–56. doi: 10.1016/j.tem.2020.12.001

47. Okita N, Higami Y, Fukai F, Kobayashi M, Mitarai M, Sekiya T, et al. Modified Western Blotting for Insulin and Other Diabetes-Associated Peptide Hormones. *Sci Rep* (2017) 7(1):6949. doi: 10.1038/s41598-017-04456-4